Journal of Electroanalytical Chemistry 676 (2012) 35–39

Contents lists available at SciVerse ScienceDirect

Journal of Electroanalytical Chemistry

journal homepage: www.elsevier.com/locate/jelechem

Short Communication

Effect of surfactant on high capacitance of galvanostatically deposited MnO_2

Suhasini *, A. Chitharanjan Hegde

Electrochemistry Research Laboratory, Department of Chemistry, National Institute of Technology Karnataka, Surathkal, Srinivasnagar 575 025, India

ARTICLE INFO

Article history:
Received 15 February 2012
Received in revised form 2 April 2012
Accepted 6 April 2012
Available online 11 May 2012

Keywords:
Galvanostatic
Manganese dioxide
Cyclic voltammetry
Charge/discharge
Surfactant

ABSTRACT

Manganese dioxide has been galvanostatically deposited on stainless-steel substrate from an aqueous acidic solution of manganese sulphate (1 M) in presence of a surface active agent (surfactant), namely, sodium lauryl sulphate (SLS), for supercapacitor applications. The deposits have been developed under different conditions of SLS and their specific capacitance is measured by cyclic voltammetry (CV) and also by galvanostatic charge/discharge cycle. The oxide film ($\sim$0.1 mg cm^{-2}) anodized from the manganese solution at 2.0 mA cm^{-2} has shown the highest specific capacitance of 255.8 F g^{-1}, at scan rate of 10 mV s^{-1}. It is observed that the capacitance increased by about 40% compared to the oxide prepared in the absence of SLS. Improved specific capacitance is due to the effect of the surfactant molecules in the deposit, causing high surface area of the deposit. The deposit is found to display good cycleability, even up to 1500 cycles. The structure and surface morphology of the deposits have been studied by means of X-ray diffraction (XRD) analysis and Scanning Electron Microscopy (SEM). XRD study reveals that crystallinity of the deposit with SLS remains unchanged, both are amorphous in nature. The surface area of the deposit is found to increase considerably due to the effect of SLS, as evident by SEM study.

© 2012 Elsevier B.V. All rights reserved.

1. Introduction

Growing environmental concerns and fast depletion of fossil fuels have created great interest in studying alternative energy sources. Electrochemical capacitors (ECs) also known as supercapacitors or ultracapacitors, have become alternative energy storage systems for applications involving high power requirements for a short duration such as camera flash equipment, pulsed light generators, fire/smoke alarms, backup power source for computer memory, purification of salt water, etc. [1–6].

The supercapacitors have high power and energy density, very long cycle lives, short charge time, high safety and high efficiency [5,7,8]. Based upon their charge-storage mechanisms, supercapacitors can be classified into two types of capacitors: (i) the non-faradic electric double layer capacitors (EDLCs), in which the capacitance arises from the charge separation at an electrode–electrolyte interface and (ii) the faradic pseudo-capacitors (PC), where the capacitance arises from the redox reactions of the electrochemically active material [9,10].

The most widely used active electrode materials are carbon (EDLCs) [11–13] conducting polymers [14,15] and both noble and transition-metal oxides (PC) [1,2,7,9,16–19]. Until now, one of the best electrode materials for electrochemical supercapacitor is ruthenium oxide [16,20,21]. However, it has the inherent disadvantage of being both expensive and toxic, which has limited its commercial use. Recently, the natural abundance and low cost of manganese oxide, accompanied by its satisfactory capacitive behaviour in mild electrolytes and environmental compatibility, have made it one of the most promising electrode materials for supercapacitors. The preparation methods of manganese oxide for supercapacitor applications include thermal decomposition, co-precipitation, sol–gel processes, physical vapour deposition, hydrothermal synthesis and anodic/cathodic deposition. It has been confirmed that the preparation methods and/or condition could significantly affect the material characteristics of the obtained manganese oxides, and thereby their pseudo-capacitive performance [22].

Generally, the physical and morphological properties of electrodeposited materials depend on the experimental conditions used for their preparation, which include the presence of foreign molecules in the electrolyte. Surfactants possess a polar head group attached to a long chain aliphatic non-polar tail. The head group can get adsorbed on the electrode surface and, therefore, can influence the double layer properties, kinetics and mechanism of electrochemical processes [1,23].

In this paper, the manganese dioxide was deposited galvanostatically, by the electrolysis of an acidic solution of $MnSO_4{\cdot}H_2O$. Oxidation of Mn^{+2} ions results in a deposit of MnO_2, which generally possess a γ-crystallographic structure or is amorphous in nature [1,23–25]. The product formed at the cathode is usually the hydrogen gas due to the reduction of H_3O^+ ions [26]. From literature, a nanostructured MnO_2 deposited on stainless-steel by electro oxidation method generally shows the capacitance in the

* Corresponding author. Tel.: +91 9743293223; fax: +91 824 2474033.
E-mail address: suni7676@yahoo.co.in (Suhasini).

1572-6657/$ - see front matter © 2012 Elsevier B.V. All rights reserved.
http://dx.doi.org/10.1016/j.jelechem.2012.04.002

range of 70–160 F g^{-1}, using manganese sulphate solution as electrolyte [27,28]. The aim of the present study is to electrochemically deposit MnO_2 in the presence of a suitable surface-active agent and to evaluate the electrodes for capacitor properties. Accordingly, MnO_2 electrodeposited in the presence of sodium lauryl sulphate (SLS) has shown that the specific capacitance varies in the range of 200–255.8 F g^{-1} against 155.4 F g^{-1} obtained for MnO_2 deposited in the absence of SLS.

2. Materials and methods

2.1. Electrodeposition of MnO_2 films

The electrolytic solutions were freshly prepared from distilled water. Analytical grade reagents ($MnSO_4{\cdot}H_2O$, $C_{12}H_{25}NaOSO_3$, and Na_2SO_4) were used in the present study. An aqueous solution of 1 M $MnSO_4{\cdot}H_2O$ in 0.15 M H_2SO_4 was prepared. A rectangular PVC cell containing 100 cm^3 electrolyte was used for deposition. For the deposition of MnO_2 in the presence of the surface active agent, the required quantity of SLS was added, followed by a thorough stirring of the electrolyte to obtain a clear solution. Experiments were carried out using different amounts of SLS up to 5 g l^{-1} in the electrolyte, but at 5 g l^{-1} SLS concentration, no clear deposition was observed. There was no much difference in capacitance up to 0.8 g l^{-1} SLS, at 1 g l^{-1} it shows maximum capacitance. The variation of capacitance with SLS concentration is shown in Fig. 1. Since the appropriate amount of SLS was found to be 1 g l^{-1}, a majority of the studies were carried out at this concentration. All depositions were carried out under the same conditions of stirring without purging, to maintain a mass transport steady-state. Anodic deposition was carried out on pre-cleaned stainless steel (SS, grade-304) panels of (10 × 3.0 × 0.1 cm) size with exposed area 7.5 cm^2. An identical, stainless steel panel was used as cathode. The electrolytic deposition of MnO_2 was carried out galvanostatically at a current density of 2 mA cm^{-2} for 5 min, using high precision power source (N6705A, Agilent Technologies). All depositions were carried out under identical conditions of pH, 1.2 ± 0.1; temperature, 30 ± 2 °C; and time, 5 min, for comparison purposes. Subsequent to deposition, the electrode was separated from the cell, rinsed with distilled water, dried at 150 °C, and weighed.

Electrochemical data were obtained with a potentiostat/galvanostat (Gamary, G750) and, in order to obtain the mass of MnO_2 films, a balance (Mettler Toledo, AL54 CEN315) was used. Electrochemical characterisation was done in a three electrode configuration cell, having 0.1 M aqueous solution of Na_2SO_4 as the electrolyte. The MnO_2 coated SS was used as a working electrode. CV measurements were performed between 0.0 V and 0.9 V (vs. Saturated Calomel Electrode) at scan rates from 10 to 150 mV s^{-1}. It was clear from Fig. 2, as scan rate increases, capacitance decreases. As counter-electrode, a 10 cm^2 platinum sheet was used. The powder X-ray diffraction (XRD) patterns of the samples were recorded using JEOL JDX-8P diffractometer using Cu Kα (λ = 1.5418 Å) as source. The surface morphology of electrodeposited MnO_2 images was recorded using a JEOL JSM-6380LA Scanning Electron Microscopy (SEM).

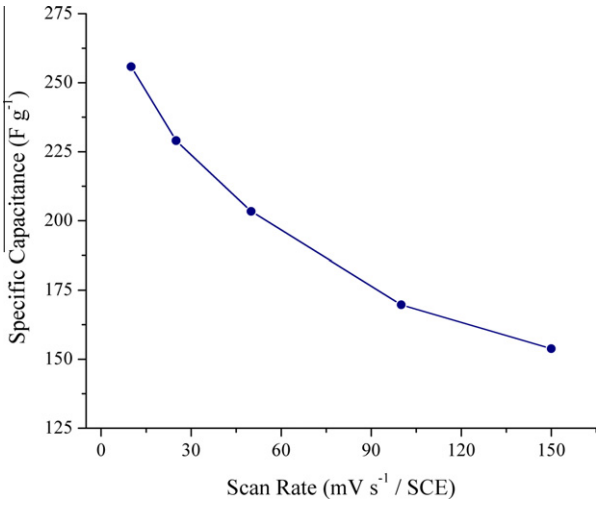

Fig. 2. Dependence of specific capacitance of MnO_2 on the scan rate.

2.2. Electrochemical characterisation

The specific capacitance (*Cs*, in Farad, F) was calculated using half the integrated area of the CV curves to obtain the charge (*Q*, in Coulomb, C), and subsequently dividing the charge by the mass of the deposit (*m*, in grams, g) and the width of the potential window (ΔV, in Volts, V), using the following equation

$$Cs = Q/m\Delta V \quad (1)$$

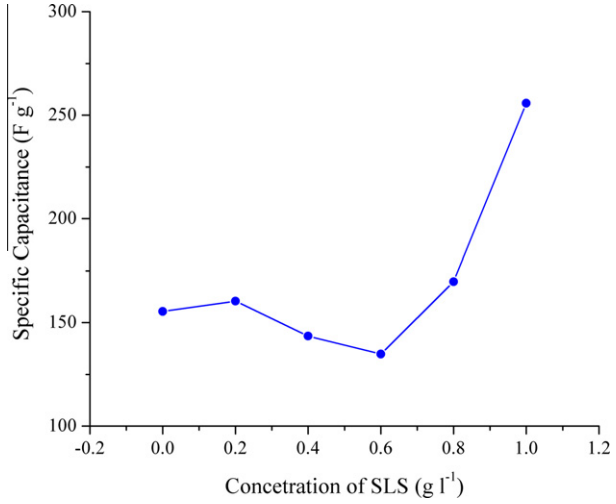

Fig. 1. Dependence of specific capacitance of $MnO_{2(s)}$ on the concentration of SLS in 1 M $MnSO_4$ solution.

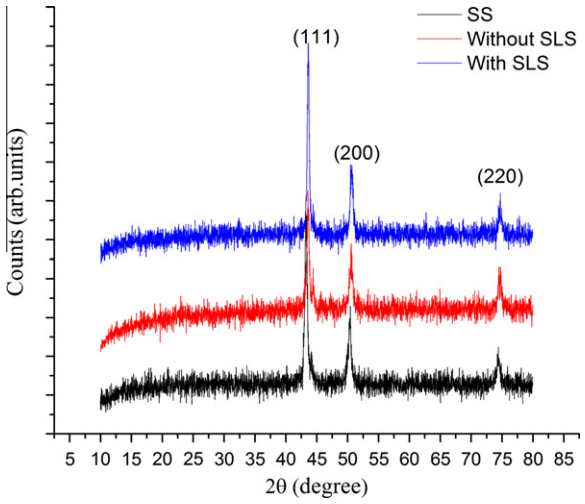

Fig. 3. X-ray diffraction patterns of bare SS and galvanostatically deposited MnO_2 and $MnO_{2(s)}$ (2 mA cm^{-2}).

Galvanostatic charge/discharge cycling was carried out at constant current density 0.5 mA cm^{-2}. Obtained charge/discharge curves were used for the calculation of *Cs* (F) from the following equation

$$Cs = I/(dV/dt)m \quad (2)$$

where *dV/dt* (V/s) is the slope of the linear discharge curve, and *I* (mA cm^{-2}) is the current density.

3. Results and discussion

The electrochemical preparation of MnO_2 from an aqueous solution contained Mn^{+2} salts has been extensively studied and reported. The reaction occurs according to,

$$Mn^{+2} + 2H_2O \rightarrow MnO_2 + 4H^+ + 2e^- \quad (3)$$

MnO_2 thus formed usually deposits as a film on the anode [1,23,26,29]. A large variety of studies on electrodeposition of MnO_2 from acidic electrolytes has been reported [9,24]. These studies have been carried out using an inert electrode such as Pt. However it is imperative to employ an inexpensive substrate instead of an expensive Pt group metal for a cost-effective application. For this reason, in the present study, SS was used as the substrate for the deposition of manganese oxide. Ni can be also used as substrate [23]. The advantage of using SS over Ni substrate is that, in acidic medium Ni undergoes oxidation and hence undergoes corrosion. In this work, the experimental setup used for deposition of MnO_2 was simple two electrode system, but the values obtained for capacitance and cycle lives were quite good. A mixed acidic aqueous solution of 1 M $MnSO_4{\cdot}H_2O$ + 0.15 M H_2SO_4 was used with increasing amounts of SLS from 0 to 5 g l^{-1}. Generally, electrolytic manganese dioxide (EMD) was deposited in acidic electrolytes consisting of a Mn^{+2} ions, using an inert electrode as anode. The oxides deposited from a solution in absence and in presence of SLS surfactant are hereafter referred to as MnO_2 and $MnO_{2(s)}$, respectively.

It is known that MnO_2 exists in several crystallographic forms [30], and an oxide prepared by electrochemical oxidation in acidic electrolytes, which is generally called the EMD, has either the γ

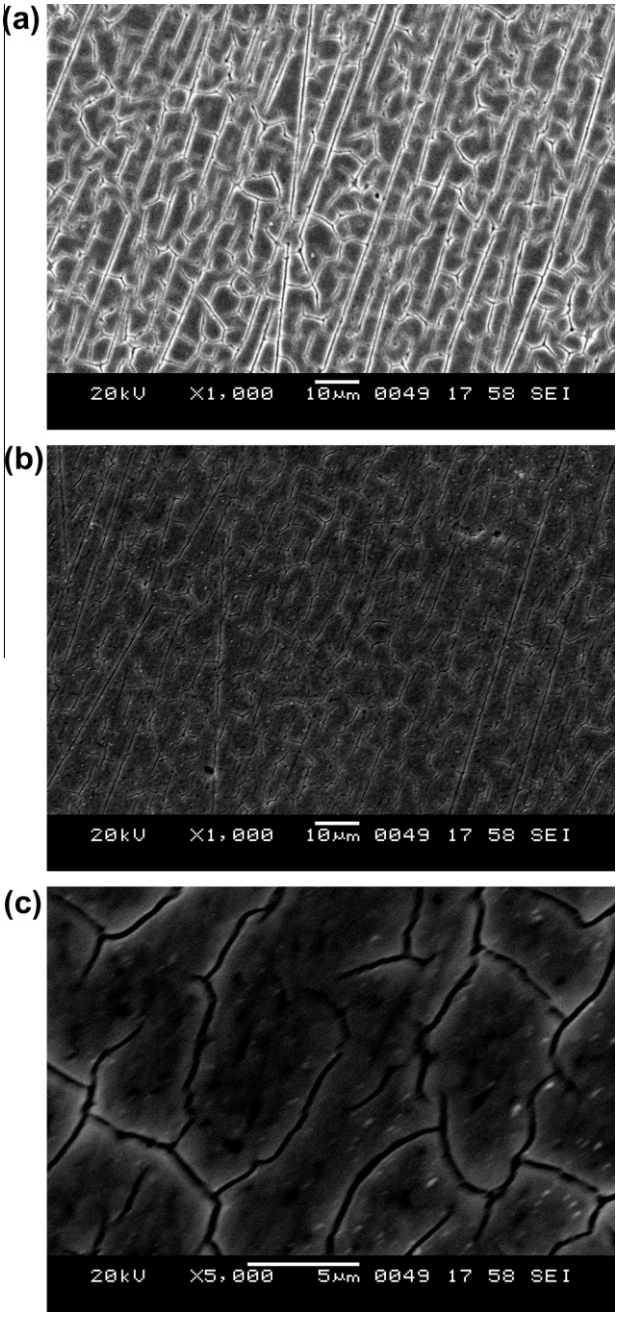

Fig. 4. SEM images of (a) MnO_2, (b) $MnO_{2(s)}$ and (c) $MnO_{2(s)}$ magnified films deposited galvanostatically at current density of 2 mA cm^{-2}.

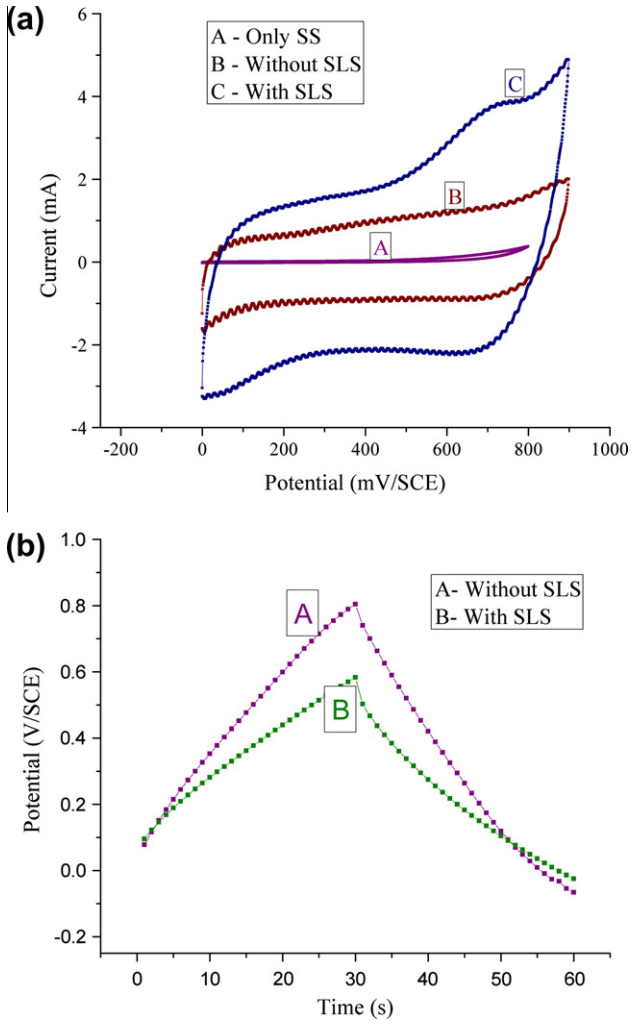

Fig. 5. (a) CV curves of the MnO_2, $MnO_{2(s)}$ and SS in 0.1 M Na_2SO_4 solution at 10 mV s^{-1} scan rate, (b) charge–discharge curves at 0.5 mA cm^{-2}.

structure or amorphous in nature. In order to examine the effect of the presence of surfactant in the solution, the XRD patterns of the bare SS, MnO_2 and $MnO_{2(s)}$ were recorded, is as shown in Fig. 3. Since XRD pattern of bare SS, MnO_2 and $MnO_{2(s)}$ were same and no peak corresponds to any of the crystalline form of MnO_2 [30]. Thus both, MnO_2 and $MnO_{2(s)}$, are amorphous in nature. From the SEM micrographs (provides morphological effect of surfactant on surface) Fig. 4a and b, it is seen that the surface of $MnO_{2(s)}$ appears rough, suggesting the higher surface area than the smoother surface of MnO_2. The important aspect seen in these images is the "cracked mud" appearance of the films as clearly observed in Fig. 4c at higher magnification. The cracking is the important factor, which enhances the cycle lives by facilitating the expansion/contraction process [31].

The charge storage mechanism in MnO_2, which has been previously reported [17], is due to a redox reaction, which also involves insertion of cations from the electrolyte into the MnO_2 lattice. The kinetics of reversible insertion/extraction of the cation varies with the electrolytes; a solution of 0.1 M Na_2SO_4 was the better electrolyte for all characterisation studies [23]. It was observed that the insertion of cation also depends on scan rates, as scan rate increases, capacitance decreases. At slow scanning rate, protons or cations have enough time to arrive at the surface of MnO_2 and to insert into the voids in MnO_2 lattice, and thus more charge can be stored. At fast scanning rate, protons and cations may not have enough time to intercalate into the voids, thus amount of charge stored by intercalation was comparatively less. It was found that the 1 g l^{-1} SLS in 1 M $MnSO_4{\cdot}H_2O$ shows maximum, appropriate capacitance. Thus $MnO_{2(s)}$ electrodes prepared out of 1 M $MnSO_4{\cdot}H_2O$ + 0.15 M H_2SO_4 + 1 g l^{-1} SLS electrolyte was used for the characterisation studies. The results of cyclic voltammetry for these studies were also confirmed by galvanostatic charge/discharge studies.

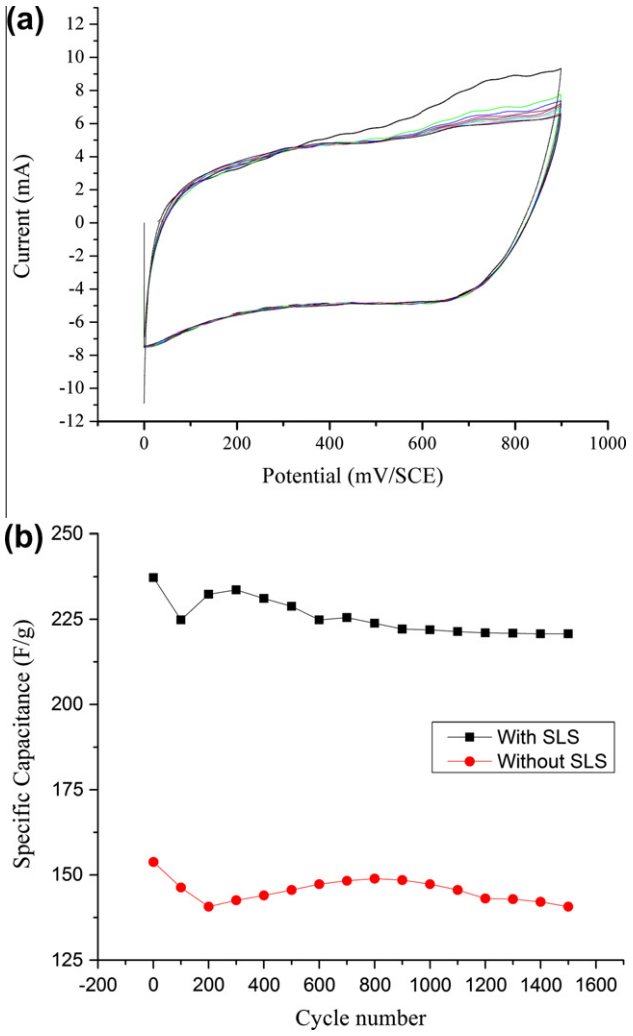

Fig. 6. (a) CV for $MnO_{2(s)}$ at 25 mV s^{-1} in 0.1 M Na_2SO_4 for cycle life, (b) cycle life data for MnO_2 and $MnO_{2(s)}$ at 25 mV s^{-1} scan rate in 0.1 M Na_2SO_4.

Cyclic voltammograms in 0.1 M Na_2SO_4 of MnO_2 and $MnO_{2(s)}$ electrodes and also bare SS electrode, for comparison, are as shown in Fig. 5a. There is no significant charge density on the bare SS electrode, thus suggesting that the contribution of the substrate to the measured capacitance of MnO_2 or $MnO_{2(s)}$ is negligibly small. The specific capacitance is (*Cs*) for MnO_2 and $MnO_{2(s)}$ are 155.4 and 255.8 F g^{-1}, respectively, at the scan rate of 10 mV s^{-1}. Thus, there is an increase of *Cs* by about 40% for $MnO_{2(s)}$ in comparison with MnO_2.

The electrodes were subjected to galvanostatic charge/discharge cycling at current density of 0.5 mA cm^{-2} is shown in Fig. 5b. The linear variation of potential during both charging and discharging process is another criterion for capacitance behaviour of material in addition to exhibiting rectangular voltammograms [8]. There is a linear variation of the potential during charge and discharge regions for both MnO_2 and $MnO_{2(s)}$. The *Cs* values obtained from the discharge data for MnO_2 and $MnO_{2(s)}$ are 154.8 and 244.0 F g^{-1}, respectively.

Both MnO_2 and $MnO_{2(s)}$ electrodes were subjected to an extended cycle-life test with CV at 25 mV s^{-1} scan rate and the variation of specific capacitance with cycle number is shown in Fig. 6a. It is seen that the specific capacitance of MnO_2 is 153.8 F g^{-1} during the initial stages of cycling. This value agrees with the studies reported in the literature. There is a decrease in capacitance on cycling and for $MnO_{2(s)}$, a *Cs* of 237.2 F g^{-1} is obtained during the initial cycles, it decreases to 220.7 F g^{-1} at 1500th cycle. The variation of *Cs* with cycle number is shown in Fig. 6b.

4. Conclusion

In order to improve the specific capacitance, amorphous MnO_2 has been electrodeposited from an acidic aqueous solution consisting of SLS as the surfactant. The electrodeposited films of MnO_2 in the presence of the surfactant possess rough surface, and hence surface area, in relation to the films prepared in the absence of the surfactant, also surfactant may facilitate the insertion of cations into the MnO_2 moiety. Cyclic voltammetry and galvanostatic charge–discharge cycling experiments reveal that the *Cs* is higher by about 40% due to the effect of SLS. It has been found that 1 g l^{-1} SLS in 1 M $MnSO_4{\cdot}H_2O$ solution is the optimum concentration for obtaining maximum *Cs*.

Acknowledgement

Suhasini is grateful to NITK, Surathkal, for providing the Institute Fellowship that allowed carrying out this work.

References

[1] S. Devaraj, N. Munichandraiah, J. Electrochem. Soc. 154 (2007) A901–A909.
[2] N. Nagarajan, H. Humadi, I. Zhitomisky, Electrochim. Acta 51 (2006) 3039–3045.
[3] Ying Zhang, Hengzhao Yang, J. Power Sources 196 (2011) 4128–4135.
[4] H. Ibrahim, A. Ilinca, J. Perron, Renew. Sust. Energ. Rev. 12 (2008) 1221–1250.
[5] Adrian Schneuwly, Roland Gallay, Properties and application of supercapacitors from the state-of-the-art to future trends, in: Proceeding PCIM 2000.
[6] Robert Atlas, Use of aqueous double layer ultracapacitor using hybrid CDI-ED technology for the use in hybrid battery systems, Aqua EWP, LLC 2006.

[7] Y. Zhao, Y.Y. Wang, Q.Y. Lai, L.M. Chen, Y.J. Hao, X.Y. Ji, Synth. Met. 159 (2009) 331–337.
[8] B.E. Conway, Electrochemical Supercapacitors, Kluwer, New York, 1999.
[9] Takuya Shinomiya, Vinay Gypta, Norio Miura, Electrochim. Acta 51 (2006) 4412–4419.
[10] B.E. Conway, V. Briss, J. Wojtowicz, J. Power Sources 66 (1997) 1–14.
[11] A.G. Pandolfo, A.F. Hollenkamp, J. Power Sources 157 (2006) 11–27.
[12] C. Schmitt, H. Probstle, J. Fricke, J. Non-Cryst. Solids 285 (2001) 277–282.
[13] Elzbieta Frackowiak, Francois Beguin, Carbon 39 (2001) 937–950.
[14] Marina Mastragostino, Catia Arbizzani, Francesca Soavi, Solid State Ion 148 (2002) 493–498.
[15] S.K. Tripathi, Ashok Kumar, S.A. Hashmi, Solid State Ion 177 (2006) 2979–2985.
[16] Yong-Qing Zhao, Guo-Qing Zhang, Hu-Lin Li, Solid State Ion 177 (2006) 1335–1339.
[17] Mathieu Toupin, Thierry Brousse, Daniel Bélanger, Chem. Mater. 16 (2004) 3184–3190.
[18] Qinghua Huang, Xianyou Wang, Jun Li, Electrochim. Acta 52 (2006) 1758–1762.
[19] N. Nagarajan, I. Zhitomirsky, J. Appl. Electrochem. 36 (2006) 1399–1405.
[20] Bong-Ok Park, C.D. Lokhande, Hyung-Sang Park, Kwang-Deog Jung, Oh-Shim Joo, J. Power Sources 134 (2004) 148–152.
[21] V.D. Patake, C.D. Lokhande, Oh-Shim Joo, Appl. Surf. Sci. 255 (2009) 4192–4196.
[22] Jeng-Kuei Chiung, Chiung-Hui Huang, Wen-Ta Tsai, Ming-Jay Deng, I-Wen Sun, Po-Yu Chen, Electrochim. Acta 53 (2008) 4447–4453.
[23] S. Devaraj, N. Munichandraiah, Electrochem Solid-State Lett. 8 (2005) A373–A377.
[24] S. Devaraj, N. Munichandraiah, Electrochem. Solid-State Lett. 12 (2009) F21–F25.
[25] D.E. Simon, R.W. Morton, J.J. Gislason, Adv. X-ray Anal. 47 (2004) 267–280.
[26] Prasant Kumar Nayak, N. Munichandraiah, Electrochem. Solid-State Lett. 12 (2009) A115–A119.
[27] S. Devaraj, N. Munichandraiah, J. Solid State Electrochem. 12 (2008) 207–211.
[28] E. Beaudrouet, A. Le Gal La Salle, D. Guyomard, Electrochem. Acta 54 (2009) 1240–1248.
[29] Shulei Chou, Fangyi Cheng, Jun Chen, J. Power Sources 162 (2006) 727–734.
[30] S. Devaraj, N. Munichandraiah, J. Phys. Chem. C 112 (2008) 4406–4417.
[31] J.N. Broughton, M.J. Brett, Electrochim. Acta 50 (2005) 4814–4819.